Journal of Hydraulic Structures
J. Hydraul. Struct., 2024; 10(1):106-118
DOI: 10.22055/jhs.2024.19077

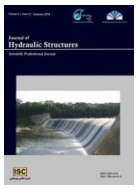

OPEN ACCESS

Numerical investigation on the hydraulic parameters' effects on the circular-crested weir

Mahdi Majedi Asl [*1]
Hadi Arvanaghi [2]
Mehdi Fuladipanah [3]
Omid Ghasemzadeh [1]
Tohid Omidpour Alavian [1]

Abstract

A paramount determinant in the selection of irrigation canal overflow configurations resides in their flow conveyance capacity. This overflow capacity is contingent upon the effective length and geometric characteristics of the weir. In the present investigation, the hydraulic performance and discharge coefficient (C_d) of circular-crested weir were scrutinized through the utilization of FLUENT software. Specifically, the study delved into the impact of geometric parameters, namely the radius and height of the crest, on these hydraulic aspects. Following the execution of calibration and validation procedures using FLUENT in conjunction with laboratory-derived data, the outcomes of the simulation revealed that augmenting the radius of the crest led to a corresponding escalation of 144.28% in the maximum pressure exerted on the crest and a 6.84% increase in flow depth. Conversely, the maximum velocity and C_d experienced reductions of 6.84% and 7.82%, respectively. The elevation of the weir height exhibited negligible influence on the maximum pressure magnitude at the crest. Contrastingly, a reduction in weir height constricted the range of pressure variations on the crest, indicating a more limited domain of pressure changes. Elevating the weir height induces a notable augmentation in the maximum flow velocity at the crest by 44.36%, concomitant with a reduction in both the depth and C_d by 52.66% and 68.96%, respectively.

Keywords: Weir Height, Circular Crest Weir, Crest Radius, Discharge Coefficient, Numerical Model.

Received: 09 November 2023; Accepted: 16 April 2024

[*] Email: mehdi.majedi@gmail.com **(Corresponding Author)**
[1] Department of Civil Engineering, Faculty of Engineering, University of Maragheh, Maragheh. Iran.
[2] Department of Water Sciences and Engineering, Tabriz University, Tabriz, Iran.
[3] Department of Civil engineering, Ramhormoz Branch, Islamic Azad University, Ramhormoz, Iran.

1. Introduction

In presenting solutions for hydraulic issues, understanding the behavior of problem-causing phenomena plays a crucial role in addressing and controlling them. One of the longstanding challenges that humanity grapples with is the issue of water scarcity. Acquiring knowledge and examining hydraulic issues, as well as understanding the behavior of water flow, greatly aids engineers in the precise design and implementation of projects in contributing to measuring flow, reducing water losses, and enhancing water resource preservation and protection. The structures for measuring and controlling flow are among the most critical components of irrigation and drainage networks. Measuring the volume of flow is vital for agricultural purposes and irrigation projects. Therefore, various methods are employed to measure the flow rate in open channels. One of the primary structures for flow measurement in open channels is the weir, utilized for the passage of water flow from the upstream to the downstream of the channel. One key consideration in selecting the type of weir is its capacity. Since the weir capacity is a function of the effective crest length and geometric shape, extensive studies have been conducted in this regard. Weirs with circular and cylindrical crests find application in the measurement, conveyance, and passing of flow in irrigation networks and water convenience systems, as their design significantly influences the weir capacity. Heidarpour and Chamani (2006) proposed an analytical model based on the non-rotational and non-viscous flow equations to predict the discharge coefficient and velocity profile. It was evaluated using experimental results, demonstrating a good agreement between the model outcomes and experimental data. They concluded that the flow over a circular-crested weir can be treated similarly to non-rotational and non-viscous flow around a cylinder. Heidarpour et al. (2008) investigated the hydraulic of the flow over a semi-circular cylinder weir and provided accurate relationships for velocity distribution on the weir crest and the pressure correction coefficient. Bagheri and Heidarpour (2010) utilized Euler's equations to determine the Cd of flow over circular-crested weir models with varying heights and radius. Their results demonstrated that the proposed relationship for estimating the Cd could be effectively generalized for different parameters of circular-crested weirs. Using the potential flow theory and applying the velocity correction coefficient in the weir crest section, they derived analytical relationships for the Cd and velocity and pressure profiles on the crest of circular-crested weirs. Shabanlou et al. (2013) examined experimentally the influence of the upstream wall slope angle on the Cd and the amount of energy loss in the flow over circular-crested weirs. Their results indicated that the upstream slope has a negligible effect on the Cd and energy dissipation. Moreover, an increase in the upstream slope angle led to a more uniform velocity distribution in the vicinity of the weir crest. Kabiri Samani and Bagheri (2014) conducted an investigation on the hydraulic of the flow over circular-crested weirs to determine the Cd and velocity distribution. According to their findings, inertial forces cause the deflection of flow lines over the circular-crested weir. Mohammadzadeh-Habili et al. (2016) examined the characteristics of flow over a wide-lipped weir with flat and quarter-circle crests. Their results revealed that the flow lines pass parallel to the crest through the wide edge of the flat-crested weir to downstream. Flow separation occurs at the beginning of the crest, leading to a potential for cavitation in this area. By introducing a quarter-circle crest and inducing curvature in the flow lines, the separation is significantly controlled, eliminating the risk of cavitation. Additionally, the Cd increases in this configuration. Haghiabi et al. (2018) investigated the velocity distribution and Cd of flow over cylindrical weirs. Through a series of experiments, they presented relationships for determining the Cd and velocity distribution in the vicinity of the weir crest. Tullis et al. (2019) conducted experiments on semi-circular and quarter-circular crested weirs with varying flow rates to examine the effect of crest shape on the Cd. The magnitude of discharge variations in the semi-circular crested weir was found to be less than that

in the quarter-circular configuration. Chanson (2020), in a study on the characteristics and stability of flow over circular weirs, observed fluctuations in the water surface during the downstream transition and separation from the weir surface, resulting in some negative pressures at these points. Consequently, it was suggested to implement aeration near the downstream region of this type of weir. Parsaie and Haghiabi (2021) endeavored to establish relationships for determining the Cd of flow over circular-crested weirs using Monte Carlo methods. Their proposed relationships, after validation with experimental data, demonstrated high accuracy in estimating the Cd of flow over weirs. In a subsequent study, Parsaie et al. (2022) investigated the impact of the Cd on the ratio of upstream flow height to weir crest radius through both experimental and numerical simulation using FLOW-3D software. Their findings reported that an increase in flow velocity leads to a reduction in pressure when the flow is high. Omidpour Alavian et al. (2022) modeled and evaluated the discharge coefficient of arched labyrinth weirs. Omidpour Alavian et al. (2022) compared the hydraulic efficiency of labyrinth weirs with quarter-circle and semi-circle crest shapes. Majedi et al. (2023) investigated the hydraulic efficiency of labyrinth weirs with quarter-circle and semi-circle crest shape. Majedi et al. (2023) compared the hydraulic efficiency of labyrinth weirs with artificial intelligence methods. In the present study, numerical simulation of circular-crested weirs has been employed to investigate the geometric effects, including the crest diameter and weir height, on the Cd of circular-crested weirs under various hydraulic conditions.

2. Materials and methods

2.1. Governing equations

The Navier-Stokes equations are the governing equations for fluid motion, adhering to the principles of momentum conservation and mass continuity for moving fluids. These equations are expressed as follows:

$$\frac{\partial \overline{u_t}}{\partial X_i} = 0 \tag{1}$$

$$\frac{\partial \overline{u_t}}{\partial t} + \bar{u}_j \frac{\partial \overline{u_t}}{\partial X_j} = -\frac{1}{\rho}\frac{\partial \bar{p}}{\partial X_i} + g x_i + \frac{\partial}{\partial x_i}\left(\vartheta \frac{\partial \overline{u_t}}{\partial x_j} - \overline{u_t u_j}\right) \tag{2}$$

Here u represents the flow velocity in the horizontal axis, motion in the horizontal (i) and vertical (j) directions. v represents the velocity in the vertical axis, ρ is the fluid density, g is the gravitational acceleration, and $\overline{P}$ denotes the corrected fluid pressure at various points, calculated as follows:

$$\overline{P}=P+2\rho k/3 \tag{3}$$

The fluid kinetic energy (k), the rate of kinetic energy dissipation (E), and the fluid viscosity (μ) are also calculated using equations (4), (5), and (6):

$$\frac{\partial(\rho k)}{\partial t}+\frac{\partial(u_i k)}{\partial x_i}=\frac{\partial}{\partial x_i}\left[\left(\mu+\frac{\mu_t}{\sigma_k}\right)\frac{\partial k}{\partial x_i}\right]+G+\varepsilon\rho \tag{4}$$

$$\frac{\partial(\rho\varepsilon)}{\partial t}+\frac{\partial(u_i \varepsilon)}{\partial x_i}=\frac{\partial}{\partial x_i}\left[\left(\mu+\frac{\mu_t}{\sigma_\varepsilon}\right)\frac{\partial \varepsilon}{\partial x_i}\right]+C_{1_s}\frac{\varepsilon}{k}G-C_{2_s}\rho\frac{\varepsilon^2}{k} \tag{5}$$

$$\mu_t=\rho C_\mu \frac{k^2}{\varepsilon} \tag{6}$$

2.2. Dimensional analysis

Fig. 1 illustrates the effective parameters affecting the Cd of flow over circular-crested weirs. In this figure, w represents the weir height, R is the weir crest radius, α is the upstream face slope angle, β is the downstream face slope angle, Q is the Cd, and H_1 denotes the head over the upstream energy line. Table 1 presents the hydraulic and geometric characteristics of the models.

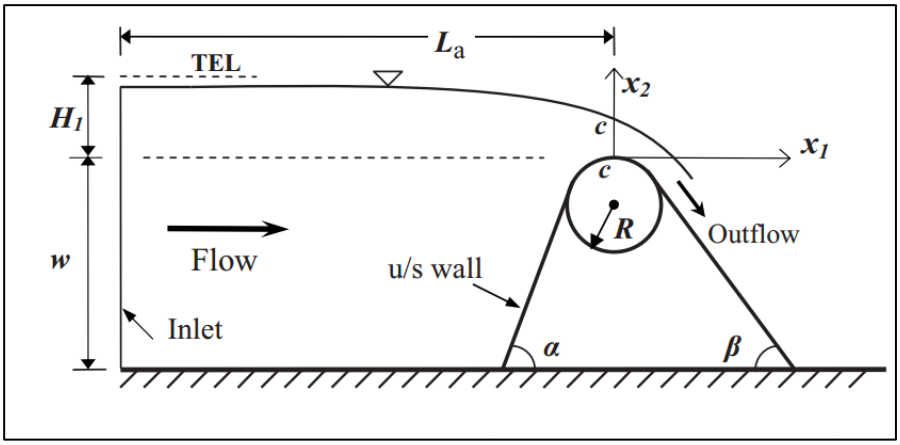

Figure 1. Schematic view of the circular-crest weir

The Cd of circular-crested weirs can be derived from the general relationship for rectangular weirs as following:

$$Q=\frac{2}{3}C_d\sqrt{2g}LH_1^{1.5} \quad (7)$$

$$C_d\frac{1.5Q}{\sqrt{2g}LH_1^{1.5}} \quad (8)$$

Herer Q represents the discharge flow rate, L is the width of the circular-crested weir, and g is the acceleration due to gravity. The relationship between the parameters influencing the Cd in the free-flow condition can be expressed as follows:

$$C_d=f(R, w, H_1, \sigma, q, g, \alpha, \beta, \rho, \mu) \quad (9)$$

By performing dimensional analysis and the Pi-Buckingham method, the dimensionless parameters are obtained as follows:

$$C_d=f(\frac{H_1}{w}, \frac{H_1}{R}, Fr, Re, We, \alpha, \beta) \quad (10)$$

Where Fr represents the Froude number, Re denotes the Reynolds number, and We stands for the Weber number. Considering that the minimum flow depth over the weir crest is greater than 0.04 meters, the influence of surface tension on the flow can be neglected. Additionally, assuming turbulent flow with Re > 10000, the viscous effects can be disregarded. Moreover, Fr is less than one in the upstream of the weir, and its variation range is small, indicating a subcritical flow regime, allowing for the neglect of its influence. Therefore, the dimensionless parameters influencing the Cd are summarized as follows.

$$C_d = f\left(\frac{H_1}{w}, \frac{H_1}{R}, \alpha, \beta\right) \quad (11)$$

Table 1. Geometry properties of the present research

Model	Weir height (m)	Weir radius (m)	Upstream slope angle	Downstream slope angle
CW1	1.16	0.15	90	90
CW2	1.16	0.15	45	45
CW3	1.16	0.20	45	45
CW4	1.16	0.10	45	45
CW5	1.50	0.15	45	45
CW6	0.60	0.15	45	45

2.3. choosing optimum mesh, turbulent model and boundary conditions

Fig. 2 depicts the schematic model along with boundary conditions. The boundary conditions of input velocity include Velocity Inlet, Pressure Inlet for air input, Pressure Outlet for the fluid surface and outlet, and a Wall condition for the flow domain walls along with the weir model. A triangular mesh is employed for model discretization, and meshes with 17586, 21560, 28842, and 34959 elements were selected for sensitivity analysis and grid independence. The obtained results are presented in Fig. 3. In this section, three turbulence models, namely k-ε (Standard), k-ε (RNG), and k-ω, were selected for the accuracy evaluation of the turbulence model. The results obtained from the water surface profile passing over the weir crest and the velocity distribution profile at the crest were compared numerically with the experimental results of Vo (1992), as shown in Fig. 4.

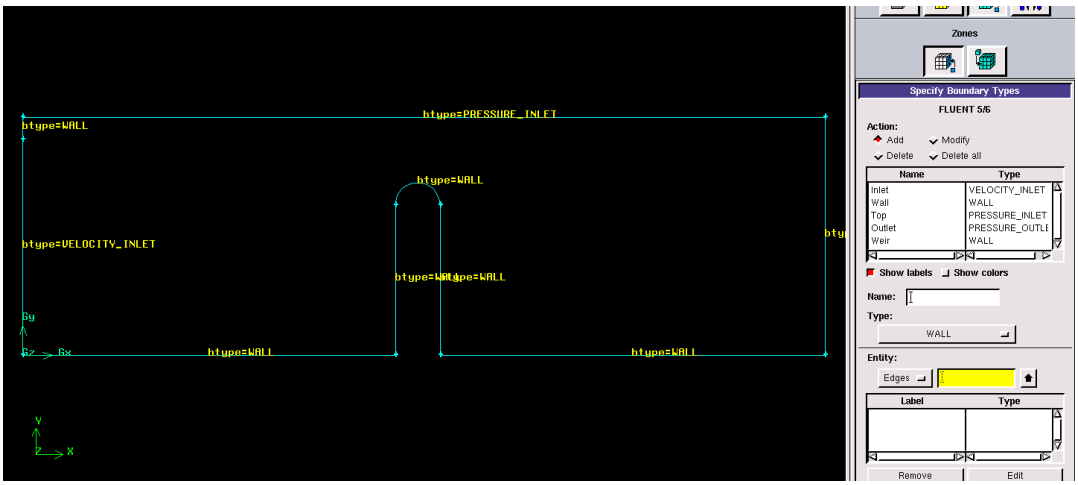

Figure 2. The definition of boundary conditions

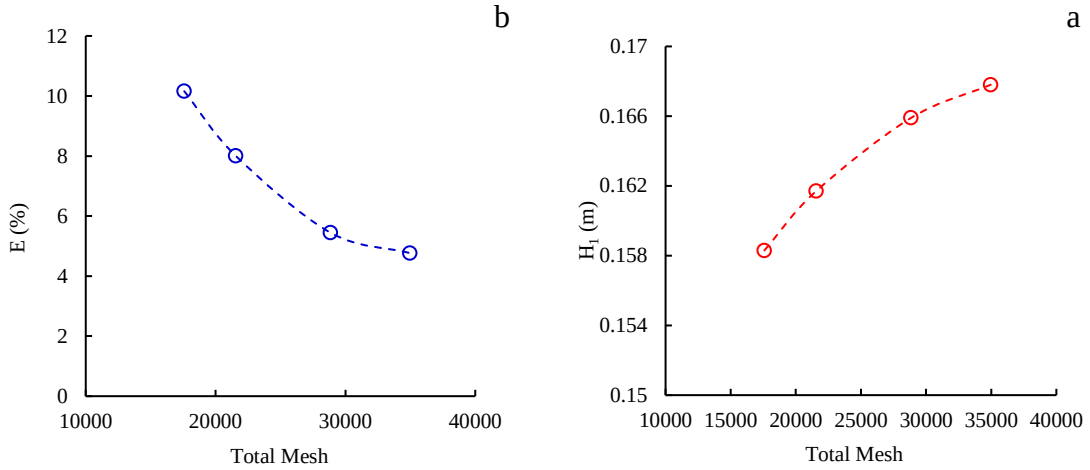

Figure 3. Optimum mesh of included models in the research

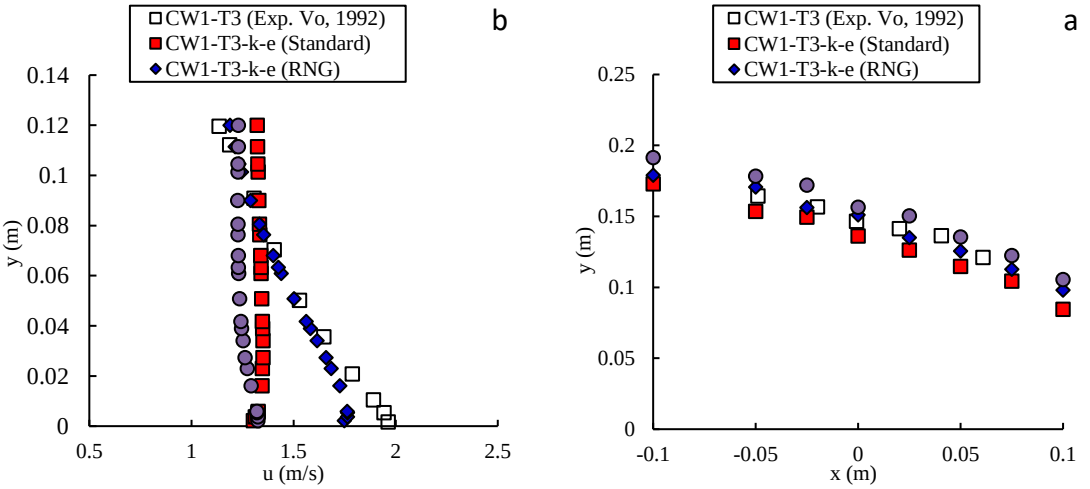

Figure 4. Comparison of (a) velocity vertical profile (b) water surface profile for included turbulent models

3. Results and discussion

The results for the optimized mesh are presented in Fig. 3. As observed, increasing in the mech number leads to a reduction in relative error percentage (E%). However, the difference in results between meshes of number 28842 and 34959 is nearly negligible. It can be concluded that the influence of the mesh size on the accuracy of the software is almost insignificant. By increasing the mesh number from 28842 to 34959, the difference in water height over the crest changes from 0.1659 to 0.1678 meters (less than 1%). Therefore, the mesh with 34959 elements can be considered as the optimal mesh. With 34959 elements, 35462 node number is corresponding to the 34959 mesh number. Referring to Fig. 4 (a and b), the results for the water surface profile and the velocity distribution over the weir crest simulation are presented. As observed, the numerical results for the water surface profile are close to the experimental results for almost all turbulence models. However, the RNG turbulence model shows better accuracy compared to the others. Additionally, by comparing the results for the velocity distribution profile, it can be observed a

slight difference between the results from the RNG turbulence model and the experimental results. Nevertheless, there is a significant difference in velocity results between the other two turbulence models and the experimental data. Table 2 presents the results of numerical simulation for various turbulence models along with the error percentage compared to experimental results. Upon careful examination of the mentioned table, it can be observed that the RNG turbulence model exhibits higher accuracy compared to the other turbulence models. On average, the relative percentage errors for k-ε (Standard), k-ε (RNG), and k-ω models for the water surface profile results are 7.62%, 3.73%, and 6.96%, respectively. Those of the velocity distribution are 15.28%, 3.55%, and 15.51%. Therefore, considering the superior output accuracy of the RNG turbulence model, it was chosen as the basis for further modeling.

Table 2. A comparison between water surface and velocity profile for turbulent models included

E-u (%)	E-h (%)	Experimental value u (m/s)	Numerical value u (m/s)	Experimental value h (m)	Numerical value h (m)	Turbulent model
31.78	0.84	1.943	1.325	0.174	0.173	
18.08	6.62	1.648	1.349	0.164	0.153	
12.05	4.61	1.528	1.344	0.156	0.149	
1.80	6.98	1.306	1.329	0.146	0.136	k-ε (Standard)
11.54	10.75	1.187	1.324	0.141	0.126	
16.42	15.94	1.135	1.321	0.136	0.114	
15.28	7.62		Mean value of relative error			
9.24	2.59	1.943	1.763	0.174	0.179	
1.97	3.92	1.648	1.615	0.164	0.171	
1.77	0.37	1.528	1.501	0.156	0.156	
1.37	3.09	1.306	1.288	0.146	0.151	k-ε (RNG)
2.25	4.48	1.187	1.213	0.141	0.135	
4.70	7.91	1.135	1.188	0.136	0.125	
3.55	3.73		Mean value of relative error			
32.01	9.75	1.943	1.321	0.174	0.191	
23.92	8.50	1.648	1.253	0.164	0.178	
19.21	9.81	1.528	1.234	0.156	0.172	
6.07	6.75	1.306	1.226	0.146	0.156	k-ω
3.54	6.35	1.187	1.230	0.141	0.150	
8.32	0.62	1.135	1.229	0.136	0.135	
15.51	6.96		Mean value of relative error			

Fig. 5 presents the results of pressure and velocity curve variations for different radii of the weir crest, including 0.1, 0.15, and 0.20 meters, with a fixed upstream and downstream slope angle (α=b=45°). It can be observed that with an increase in the weir crest radius, the pressure values on the weir crest also increase. Additionally, the pressure range on the weir crest decreases with an increase in the crest radius. For a radius of 0.1 meters, the pressure range on the weir crest is between -0.03 to 0.021 meters, whereas for radii 0.15 and 0.2 meters, it varies between 0.012 to 0.032 and 0.041 to 0.045 meters, respectively. Furthermore, the maximum pressure on the weir crest is observed to be higher for larger radii. The maximum pressure values for weir crest radii of 0.1, 0.15, and 0.2 meters are 0.021, 0.032, and 0.045 meters, respectively. Therefore, the maximum pressure on the weir crest increases by 114.28% with a twofold increase in the weir crest radius. As observed in Fig. 5-b, the velocity on the weir crest decreases with an increase in the crest radius. The reduction in velocity with an increase in the crest radius is more pronounced near the weir crest than in the flow region. The maximum velocity values for weir crest radii of 0.1, 0.15, and 0.2 meters are 2 1.77, and 1.68 meters per second, respectively. Hence, the maximum velocity on the weir crest decreases by 19.04% with a twofold increase in the weir crest radius, as depicted in Fig. 6. It is evident in Fig. 6 that the range of velocity variations on the weir crest is higher for smaller radii compared to other models.

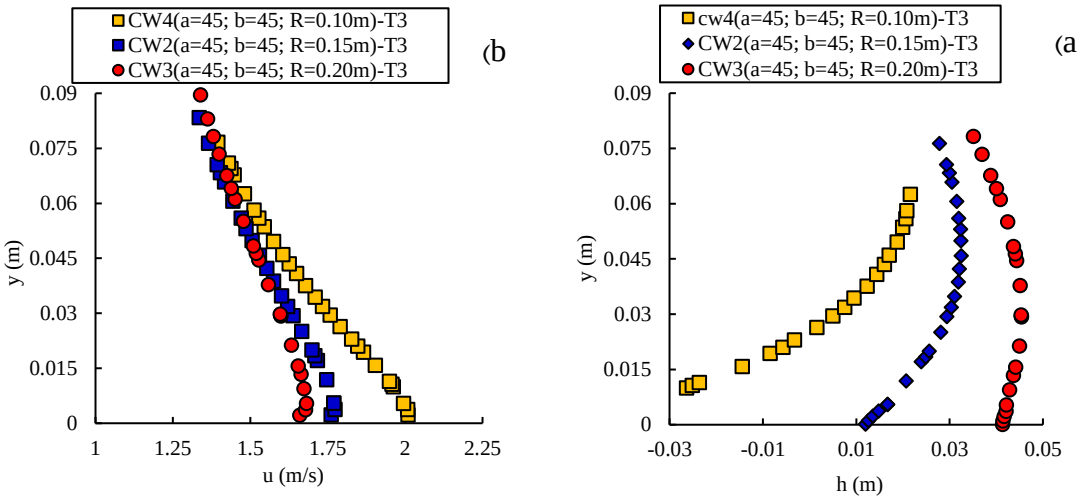

Figure 5. The effect of radius of the circular-crested weir on the (a) pressure and (b) velocity

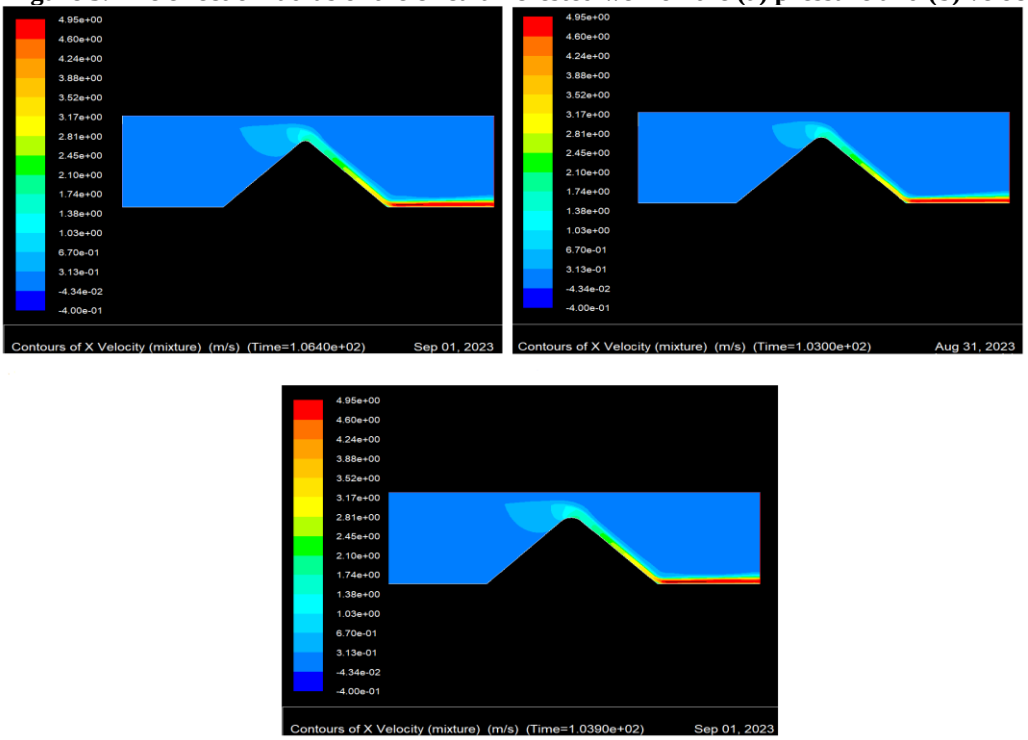

Figure 6. Flow velocity passing through circular-crested weir of radii 0.1, 0.15 and 0.2 m

Fig. 7 presents the flow surface profiles for different weir crest radii of circular-crested weir models. It is observed that with an increase in the weir crest radius, the height of the flow surface profile on the weir crest increases. In other words, as the weir crest radius decreases, the depth of the flow on the weir crest decreases. On average, with a decrease in the weir crest radius from 0.2 meters to 0.1 meters, the depth of the flow on the weir crest decreases by 6.84%.

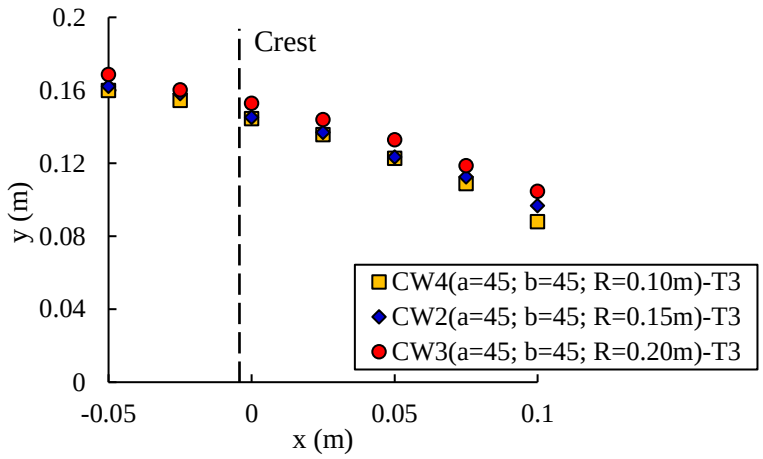

Figure 7. The effect of crest radius on the water surface profile

Fig. 8 shows the flow surface profiles for different weir crest radii for circular-crested weir models. According to this graph, an increase in the weir crest radius leads to an increase in the height of the flow surface profile on the weir crest. In other words, a decrease in the weir crest radius is equivalent to a reduction in the depth of the flow on the weir crest. On average, with a decrease in the weir crest radius from 0.20 meters to 0.1 meters, the depth of the flow on the weir crest decreases by 6.84%.

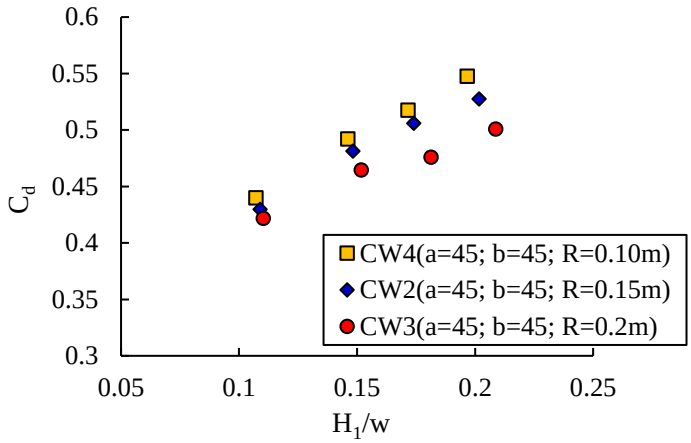

Figure 8. The variation of Cd vs. H1/W for various radii

In Fig. 9, the results of pressure and velocity curve variations are presented for different weir heights, including 0.6, 1.16 and 1.5 meters, considering a fixed upstream and downstream slope angle (α=β=45°). It is observed that the trend of the pressure distribution curve on the weir crest changes with the variation of weir height. Increasing the weir height leads to the expansion of the pressure distribution range on the weir crest, and as the weir height decreases, the range of pressure values on the crest becomes more limited. For instance, for a height of 0.6 meters, the pressure range on the crest is between -0.032 to 0.017 meters, while for heights of 1.61 and 0.5 meters, it ranges from 0.012 to 0.032 and -0.016 to 0.032 meters, respectively. The maximum pressure values on the weir crest are nearly identical for all three different weir heights, as shown in Fig. 9-

b. Additionally, the velocity on the weir crest increases with the rise in weir height, and the increase in velocity with the increase in weir height near the weir crest is more significant than the flow surface. The maximum velocity values for weir heights of 0.6, 1.61, and 1.5 meters are 1.42, 1.77 and 2.05 meters per second, respectively. Consequently, the maximum velocity on the weir crest increases by 44.36% with a two-and-a-half-fold increase in weir height. In Fig. 10, it is observed that the range of velocity variations on the weir crest and downstream is greater for larger weir heights compared to other models.

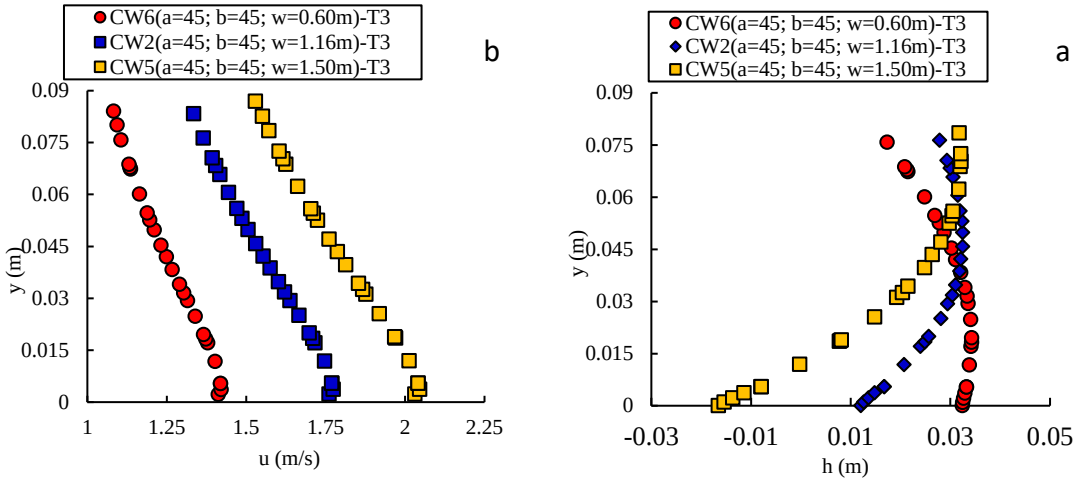

Figure 9. The effect of the weir height on the (a) pressure (b) velocity distribution

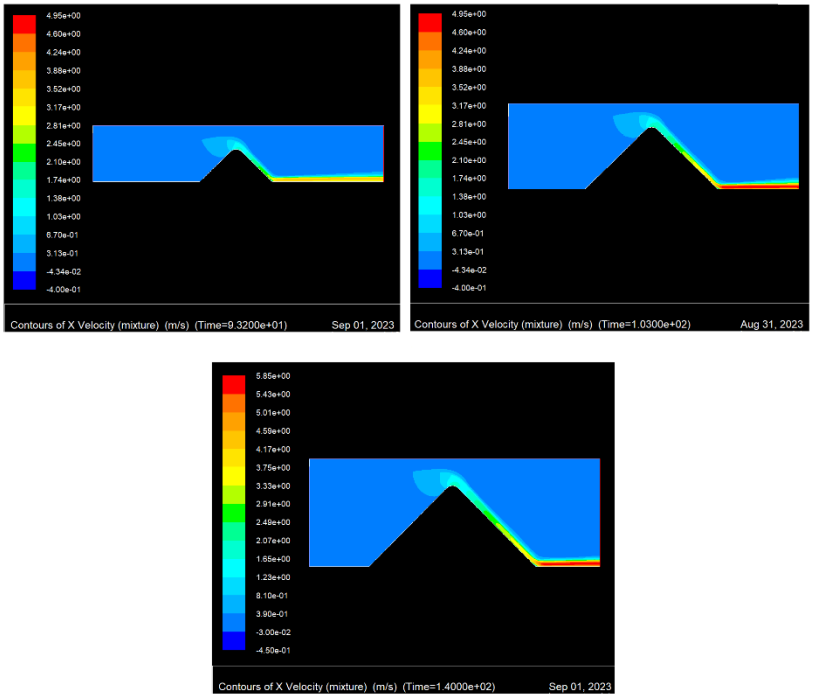

Figure 10. The passing flow velocity counter through circular-crested weir of heights 0.6, 1.16 and 1.5

Fig. 11 reveals the profiles of the flow surface over the weir crest for different weir heights. It is observed that with an increase in weir height, the height of the flow surface profile over the weir crest also increases. In other words, as the weir height decreases, the depth of the flow over the weir crest decreases. On average, with a decrease in weir height from 1.5 meters to 0.6 meters, the depth of the flow over the weir crest decreases by 52.66 %.

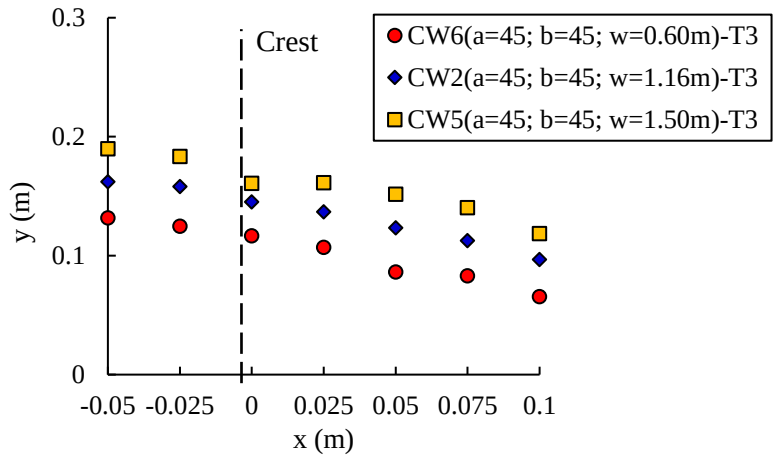

Figure 11. The effect of the weir height on the water surface profile passing through the crest

Fig. 12 illustrates the variations of the C_d for flow over circular-crested weir models with respect to weir height. It is observed that, in all models, the C_d increases with an increase in H_1/R. The main difference lies in the slope of the increasing trend of the C_d with the increase in H_1/R at different weir heights. In other words, the increasing trend of the C_d becomes steeper with a decrease in weir height. With an increase in weir height, the Cd decreases due to the increased flow depth upstream of the weir. On average, an increase in weir height from 0.6 meters to 1.50 meters results in a 68.96% reduction in the C_d.

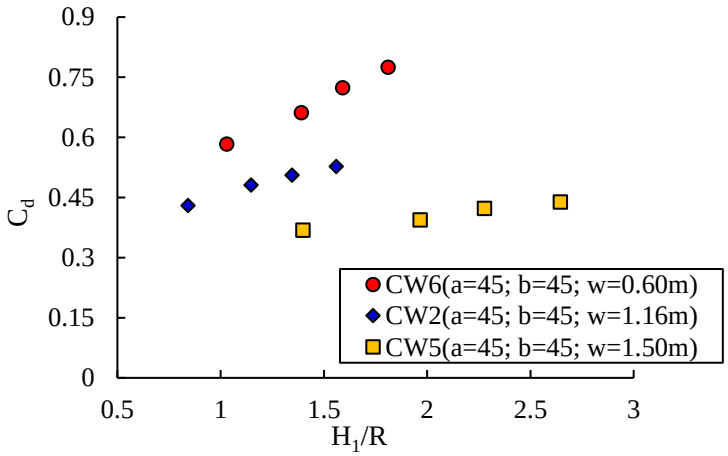

Figure 12. The variation of C_d vs. H_1/R of various weir height

4. Conclusion

This research investigates the influence of geometric parameters of circular-crested weirs, including weir's radius and height on the flow characteristics, such as pressure and velocity distribution on the crest, flow profile and Cd. Three turbulence models, namely k-ε (Standard), k-ε (RNG), and k-ω, were opted for evaluating the accuracy of the turbulence model. The results of the surface profile and depth-averaged velocity distribution from the numerical simulation of flow over the circular-crested weir were compared with experimental results. The k-ε (RNG) turbulence model exhibited higher accuracy compared to the other turbulence models. The findings indicate that:

- With a raise in the weir crest radius, the pressure values on the weir crest increase.
- The pressure range on the weir crest decreases with an increase in the weir crest radius.
- The velocity on the weir crest decreases with an growth in the crest radius.
- The velocity reduction with an increase in the crest radius is more pronounced in the vicinity of the weir crest than in the flow surface.
- By reducing the weir crest radius, the depth of the flow on the weir crest declines. On average, with a decrease in the weir crest radius from 0.2 meters to 0.1 meters, the depth of the flow on the weir crest decreases by 6.84 percent.
- With an increase in the weir crest radius, the Cd decreases. The decrease in the Cd is more noticeable in higher values of H1/w.
- On average, increasing the weir crest radius from 0.1 meters to 0.2 meters results in a 7.82 percent decrease in the Cd.

Increasing the weir crest height results in the expansion of the pressure distribution range on the crest. As the crest height decreases, the range of pressure values becomes more restricted. The maximum pressure on the crest is the same for all three different crest heights, while the velocity on the crest increases with an amplification in crest height. The velocity raise is more pronounced near the crest compared to the flow surface.

References

1. Heidarpour, M., Chamani, M. R. (2006). Velocity distribution over cylindrical weirs, Journal of Hydraulic Research, 44, 5, 708- 711.
2. Heidarpour, M., Habili, J. M., Haghiabi, A. H. (2008). Application of potential flow to circular-crested weir. Journal of hydraulic research, 46(5), 699-702.
3. Bagheri, S., Heidarpour, M. (2010). Overflow characteristics of circular-crested weirs. Journal of Hydraulic Research, 48(4), 515- 520.
4. Shabanlou, S., Khorami, E., Rajabi, A. (2013). The effects of various upstream arches of crest of the circular crested weir on hydraulic parameters. Flow Measurement and Instrumentation, 32, 103-106.
5. Kabiri-Samani, A., Bagheri, S. (2014). Discharge coefficient of circular-crested weirs based on a combination of flow around a cylinder and circulation. Journal of Irrigation and Drainage Engineering, 140(5), 04014010.
6. Mohammadzadeh-Habili, J., Heidarpour, M., Haghiabi, A. (2016). Comparison the hydraulic characteristics of finite crest length weir with quarter-circular crested weir. Flow Measurement and Instrumentation, 52, 77-82.
7. Haghiabi, A. H., Mohammadzadeh-Habili, J., Parsaie, A. (2018). Development of an evaluation method for velocity distribution over cylindrical weirs using doublet concept. Flow Measurement and Instrumentation, 61, 79-83.

8. Tullis, B. P., Crookston, B., Bung, D. (2019). Weir head-discharge relationships: A multi-lab exercise. E-proceedings of the 38th IAHR World Congress, Panama City, Panama, 1-15.
9. Chanson, H., and Montes, J. S. (1997). Overflow characteristics of cylindrical weirs. Res. Rep. No. CE 154, Dept. of Civil Engineering, University of Queensland, Brisbane, Australia.
10. Parsaie, A., Jaafer Suleiman Shreef, S., Haghiabi, A. H., Hoobi Irzooki, R., Khalaf, R. M. (2022). Numerical simulation of flow on circular crest stepped spillway. Applied Water Science, 12 (215), 1-10
11. Parsaie, A., Haghiabi, A. H. (2021). Uncertainty analysis of discharge coefficient of circular crested weirs. Applied Water Science, 11(2), 1-6.
12. Omidpour Alavian, T., and Majedi-Asl, M, Sohrabi, F, Shamsi, V. and Ayami, M. (2022c). Modeling and evaluation of the discharge coefficient of an arched Labyrinth with the Qnet met model method, the first modern national conference in civil and environmental engineering. Ramsar, Iran.
13. Omidpour Alavian, T., Majedi-Asl, M, Soltani, M, Mohammadi, E. and Shamsi, V. (2022b). Comparison of the hydraulic efficiency of Labyrinth Weirs with quarter-circle and semi-circular crest shape using met model method (ANN), 8th.International Labyrinth on Civil Engineering, Architecture and Urban Development / 07-09 March. 2023, Tehran, Iran.
14. Majedi Asl, M., Omidpour Alavian, T and Kouhdaragh, M. (2023). Comparison of The Hydraulic Efficiency of labyrinth Weirs with a Quarter and Semi-Circular Crest Shape Using Neural Networks (QNET, SVM, GEP, ANN). Iranian Journal of Irrigation and Drainage No.4, Vol. 17, Oct.-Nov. 2023, p. 787-804.
15. Majedi Asl, M., Omidpour Alavian,, Kouhdaragh, M and Shams, V. (2023).Comparison of Hydraulic Efficiency of Arched Non-linear Weirs in Plan Using GEP and SVM Neural Networks. Journal of Water and Soil Science Vol. 27, No. 3, Fall 2023, Isfahan University of Technology, Isfahan, Iran.
16. VO, N. D. (1992). Characteristics of curvilinear flow past circular-crested weirs. Ph.D. thesis, Concordia Univ., Montreal, Canada.